Standstill Determination of PM Flux Linkage Based on Minimum Saliency Tracking for PM-SyR Machines

(Article begins on next page)

Standstill Determination of PM Flux Linkage Based on Minimum Saliency Tracking for PM-SyR Machines

Paolo Pescetto
DENERG Department
Politecnico di Torino
Torino, Italy
paolo.pescetto@polito.it

Gianmario Pellegrino
DENERG Department
Politecnico di Torino
Torino, Italy
gianmario.pellegrino@polito.it

Abstract—Permanent Magnet assisted Synchronous Reluctance (PM-SyR) motors often present relevant magnetic saturation, especially if overload capabilities want to be exploited. The knowledge of current-to-flux relationship is mandatory for proper motor control, and it becomes even more critical in case of sensorless applications. Reliable self-commissioning tests have been recently developed for Synchronous Reluctance (SyR) motors without producing any rotor movements. This procedure can be extended to PM-SyR motors, but, being at standstill, it does not retrieve the flux contribution related to the PMs. This paper integrates the identification of the flux characteristic including a novel test for estimating the PM flux, obtaining the complete magnetic characteristic of PM-SyR motors. The global identification session is performed at standstill and without a position transducer, while the load can either be connected or not. These conditions are considered the most demanding for self-commissioning tests. The machine is first excited with a proper sequence of bipolar high voltage pulses to determine its current dependent flux component. Then, the PM flux linkage is retrieved at standstill by evaluating the local saliency along the negative q axis. The proposed method was experimentally verified on a 10 kW PM-SyR motor prototype, with an estimation error of 0.42%.

Index Terms—Self Commissioning, PM Flux, PMSM, PM Synchronous Reluctance Machines, Magnetic Model Identification, Flux Maps.

I. Introduction

The industrial interest in Synchronous Reluctance (SyR) motors is recently growing in a wide number of applications, mostly because of their higher efficiency and competitive torque per volume ratio respect to the Induction Motors (IM), their good overload capabilities and their generally lower price respect to the other synchronous machines based on Permanent Magnets (PM). Moreover, the high anisotropy of SyR motors makes them suitable for low speed sensorless control, which commonly exploits saliency based algorithms. The main drawbacks of SyR machines are their generally limited flux weakening capability and low power factor, which leads to inverter oversize. The addition of small amount of PM into the flux barriers, resulting in a PM-SyR motor, considerably improves both the power factor and the high speed power curve, with limited impact on the cost of the drive.

One major disadvantage of both SyR and PM-SyR machines is their highly non-linear magnetic characteristic (flux maps), presenting direct and cross saturation effects [1]. Accurate knowledge of the flux maps is mandatory for control calibration, especially in sensorless applications [2], [3]. The standard methods for inductance measurement [4] require a dedicated test rig and off-line identification of each new machine. Recently, several self-commissioning techniques were proposed [5]–[7], still most of them requiring a rotary encoder, rotor to be locked or free to rotate at sufficiently high speed. These requirements may not be respected in industrial environment, thus limiting the applicability of the methods like [6], [7]. In [8], [9] accurate standstill self-identification techniques were proposed, able to identify the complete magnetic model of SyR motors at standstill without locking the rotor and not implying position transducers, which are considered the most demanding conditions.

Standstill commissioning tests usually do not include the PM flux linkage contribution λ_{pm}, often evaluated by measuring the back-EMF voltage while the shaft rotates at open

Fig. 1. PM-SyR machine under test.

Nominal current [A]	28
Nominal dc-link voltage [V]	360
Pole pairs	2
Nominal torque [Nm]	27
Nominal speed [rpm]	2500
Maximum speed [rpm]	10000
Nominal peak power [kW]	10
Phase resistance [Ω]	0.9
Switching frequency [kHz]	10

Fig. 2. Flux maps of the machine under test.

windings. Such operation requires a prime mover and voltage transducers and it is necessarily performed off-line. Evaluating λ_{pm} at standstill is necessary, for example, in case a sensitive load is already connected to the drive or if the rotor is locked. One possible solution is to online adapt the estimated λ_{pm} during operation, as for example in [10], [11], but increasing the complexity of the motor control and/or requiring an initial estimate. Quasi-standstill methods for λ_{pm} measurement were proposed in [12]–[14]. Anyway, [12] needs a position transducer and a calibrated speed loop, so it cannot be considered sensorless, while [13], [14] require some rotor movement and free-shaft conditions.

This work extends the self-commissioning technique of [9] to PM-SyR motors, adding a novel solution for evaluating the PM flux linkage. The test is based on the evaluation of local machine anisotripy along the q-axis. Differently from [13], [14], the test is completely standstill. The complete identification stage is performed in sensorless, while the load can either be connected or not. The proposed technique is experimentally validated on a PM-SyR motor prototype, shown in Fig. 1, with accurate results.

II. MODEL OF PM-SyR MACHINES

The basic equations of the model of PM-SyR machines are briefly described here. The synchronous dq coordinates will be adopted, being the d-axis the direction of minimum reluctance on the rotor.

A. Fundamental Model

The stator voltage can be conveniently computed as:

$$\begin{cases} v_{\mathrm{d}} & = R_{\mathrm{s}}i_{\mathrm{d}} + \frac{\partial \lambda_{\mathrm{d}}}{\partial t} - \omega \lambda_{\mathrm{q}} \\ v_{\mathrm{q}} & = R_{\mathrm{s}}i_{\mathrm{q}} + \frac{\partial \lambda_{\mathrm{q}}}{\partial t} + \omega \lambda_{\mathrm{d}} \end{cases} \quad (1)$$

where R_{s} is the stator resistance. The flux linkage in each axis depends on both the dq current components, following a non-linear relationship:

$$\begin{cases} \lambda_{\mathrm{d}} & = \lambda_{\mathrm{d}}\left(i_{\mathrm{d}}, i_{\mathrm{q}}\right) \\ \lambda_{\mathrm{q}} & = \lambda_{\mathrm{q}}\left(i_{\mathrm{d}}, i_{\mathrm{q}}\right) \end{cases} \quad (2)$$

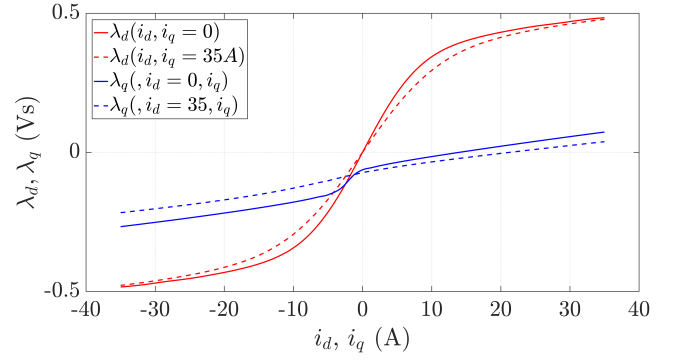This relationship is commonly called flux maps. It should be noted that, in this work, the d axis is considered the

direction of maximum inductance. As a consequence, the PM are oriented in negative q axis direction. The flux maps of the machine under test are reported in Fig. 2.

B. High Frequency Model

If the motor is excited with an High Frequency (HF) signal, the resistive voltage drop and motional terms in (1) become small in percentage respect to the flux derivative. Therefore, (1) reduces to be:

$$\begin{cases} v_{\mathrm{dh}} & \approx \frac{\partial \lambda_{\mathrm{d}}}{\partial t} \\ v_{\mathrm{qh}} & \approx \frac{\partial \lambda_{\mathrm{q}}}{\partial t} \end{cases} \quad (3)$$

where the subscript h stands for the HF component. It is useful to define the differential inductances, which determine the relationship between current and flux derivative:

$$l_{\mathrm{d}} = \frac{\partial \lambda_{\mathrm{d}}}{\partial i_{\mathrm{d}}} \qquad l_{\mathrm{q}} = \frac{\partial \lambda_{\mathrm{q}}}{\partial i_{\mathrm{q}}} \quad (4)$$

$$\begin{cases} \lambda_{\mathrm{dh}} & \approx l_{\mathrm{d}}i_{\mathrm{dh}} \\ \lambda_{\mathrm{qh}} & \approx l_{\mathrm{q}}i_{\mathrm{qh}} \end{cases} \quad (5)$$

C. PM and Armature Flux Linkage Breakdown

The $\lambda_{\mathrm{q}}(i_{\mathrm{q}})$ characteristic of PM-SyR machines includes the flux linkage component due to the PM λ_{pm}. As proposed in [13], the $\lambda_{\mathrm{q}}(i_{\mathrm{q}})$ characteristic is split into a current dependent term $\lambda_{\mathrm{q}0}(i_{\mathrm{q}})$, or armature flux, and a negative offset due to the PM:

$$\lambda_{\mathrm{q}}\left(i_{\mathrm{d}}, i_{\mathrm{q}}\right) = \lambda_{\mathrm{q}0}\left(i_{\mathrm{d}}, i_{\mathrm{q}}\right) - \lambda_{\mathrm{pm}} \quad (6)$$

where $\lambda_{\mathrm{q}0}$ is null for $(i_{\mathrm{d}} = 0, i_{\mathrm{q}} = 0)$ and λ_{pm} is a constant value. In other words, λ_{pm} is the flux linkage in q axis when the current is null:

$$\lambda_{\mathrm{q}}\left(i_{\mathrm{d}} = 0, i_{\mathrm{q}} = 0\right) = -\lambda_{\mathrm{pm}} \quad (7)$$
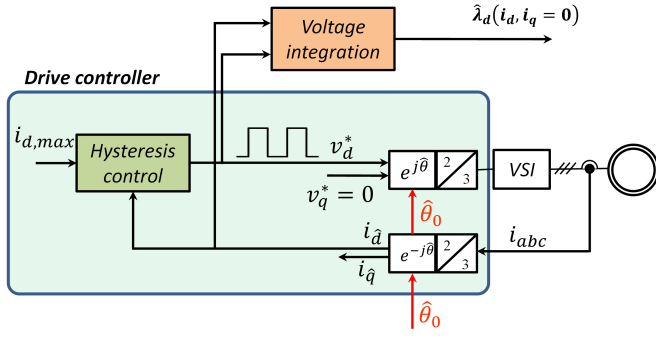
Fig. 3. Control block diagram for test #1.

III. COMMISSIONING OF THE ARMATURE FLUX MAPS

In [9], the flux maps of SyR machines are retrieved. The same method is adopted here for evaluating the current-dependent term of the flux maps (λ_d and $\lambda_\mathrm{q}0$).

At first, a standard sensorless HF injection technique is adopted to evaluate the initial rotor position $\hat{\theta}_0$. Since it is assumed that the rotor does not move during the test, $\hat{\theta}_0$ is used to define the dq directions during all the commissioning stage.

Then, a 3-step procedure is adopted. At the first stage (**test #1**), the d axis, i.e. the direction of maximum inductance, is excited with bipolar square-wave voltage, while $v_\mathrm{q} = 0$. The amplitude of the applied voltage is similar to the rated value, while its polarity is reversed when i_d overcomes a defined threshold value, according to an hysteresis mechanism. Being the d-axis only excited, torque is not produced for SyR machines, so the motor does not move, whatever the mechanical load. Fig. III shows the motor control scheme for test #1. The self-saturation flux characteristic in d axis $\lambda_\mathrm{d}(i_\mathrm{d}, i_\mathrm{q} = 0)$ is retrieved from back-EMF integration:

$$\lambda_\mathrm{d} = \int (v_\mathrm{d} - R_\mathrm{s} i_\mathrm{d})\, \mathrm{d}t \tag{8}$$

where R_s is the stator resistance and v_d is estimated from inverter commands, after compensation of inverter voltage drop.

The **test #2** is dual to the first one, but the q axis is excited with a hysteresis based square-wave voltage while $v_\mathrm{d} = 0$. The curve $\lambda_\mathrm{q}(i_\mathrm{d} = 0, i_\mathrm{q})$ is obtained, again from back-EMF integration:

$$\lambda_\mathrm{q} = \int (v_\mathrm{q} - R_\mathrm{s} i_\mathrm{q})\, \mathrm{d}t \tag{9}$$

Again, one axis only is excited, so torque is not produced for SyR machines. Anyway, this test is less stable than the previous one, since eventual inaccuracy in the estimation of $\hat{\theta}_0$ may result in drifting from the initial position. In this case, the test would fail. For this reason, test #2 can be augmented (if necessary) with online position tracking, as addressed in [15].
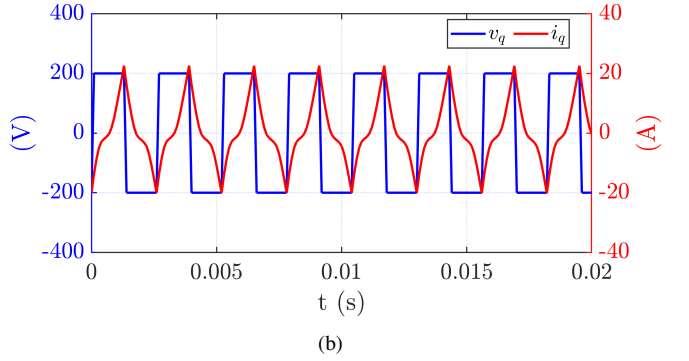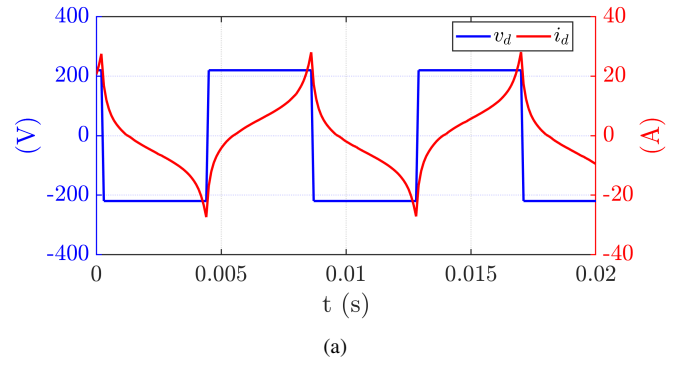

(a)

(b)

Fig. 4. Current, voltage and estimated flux waveform during test #1.

Finally, in **test #3** the two axes are contemporary excited to evaluate the cross-coupling effect. Eq. (8),(9) are simultaneously adopted to retrieve the flux maps $\boldsymbol{\lambda}_\mathrm{dq}(\boldsymbol{i}_\mathrm{dq})$ among the entire dq plane. A more detailed description of the test sequence can be found in [9].

This identification procedure, proposed in [9] for SyR machines, is now extended to the PM-SyR case. These motors present a $\lambda_\mathrm{d}(i_\mathrm{d})$ characteristic similar to an equivalent SyR machine, so the commissioning test #1 is conveniently replicated with no modification. The only additional issue is that during this test, the PM produce transient torque, which may move the rotor from its initial position. Anyway, the polarity of the torque is reversed at every current reversal, which happens at considerably high frequency (30÷50 Hz). Therefore, in free-shaft conditions the rotor may slightly vibrate, but without considerably move from its initial position. In case the transient torque is too big, so there is the risk of rotor movement, the test can be augmented with HF voltage injection for online position tracking, as addressed in [15]. The voltage and current waveforms are report in Fig. III.

Conversely, the test #2 can only provide the armature flux component $\lambda_\mathrm{q0}(i_\mathrm{q})$, without the PM contribution. Fig. 5 shows the results of the two tests on the PM-SyR motor under test. The initial state of the integrator is appropriately set to force $\lambda_\mathrm{q0}(i_\mathrm{q} = 0) = 0$. A dedicated additional test is needed to retrieve λ_pm, as proposed in the next sections.

About the test #3, the cross-saturation effect in PM-SyR machines is very similar to the SyR case, so it will not be further investigated here, being this work focused on PM flux
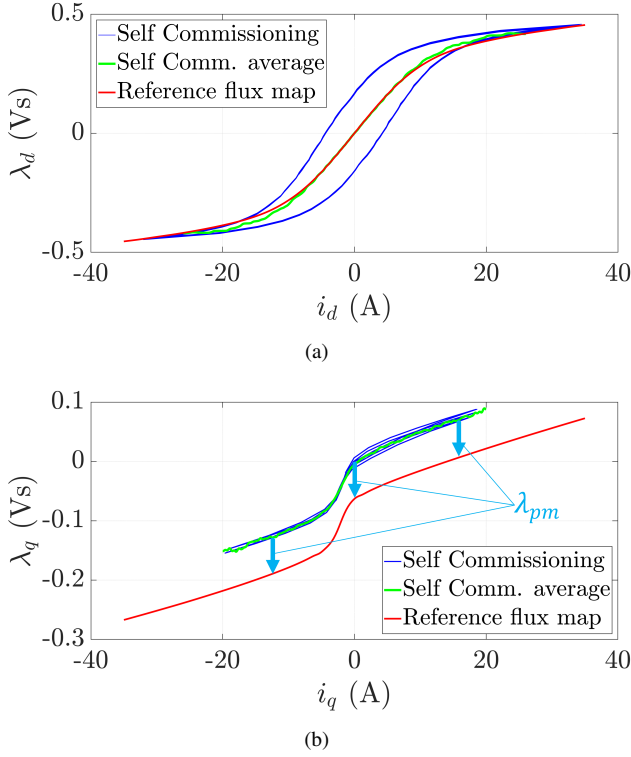
Fig. 5. Results of standstill commissioning on d and q axes.

Fig. 6. (a) Representation of zero torque locus and (b) zoom of q axis flux characteristic.

identification.

IV. PM Flux Identification at Standstill

The self-commissioning paradigm requires the identification to be at free shaft and standstill, avoiding to measure the open circuit back-emf.

A feasible solution proposed in [13] is to exploit the zero torque locus, defined as the trajectory in the dq plane where the torque is null, out of the q axis. Along this trajectory, the reluctance torque is counteracted by the torque component due to the PMs. Considering the well known formulation for the electromechanic torque:

$$T = \frac{3}{2} p \left(\lambda_{\mathrm{d}} i_{\mathrm{q}} - \lambda_{\mathrm{q}} i_{\mathrm{d}} \right) = 0 \qquad (10)$$

therefore, considering (6):

$$\left(\lambda_{\mathrm{q}0} - \lambda_{\mathrm{pm}} \right) i_{\mathrm{d}} = \lambda_{\mathrm{d}} i_{\mathrm{q}} \qquad (11)$$

This equation presents two possible solutions. The first is $i_{\mathrm{d}} = 0$ and so $\lambda_{\mathrm{d}} = 0$, which means the current vector is aligned with the magnets (q axis). This solution is not useful for determining λ_{pm}. The second solution, which can be extracted considering $i_{\mathrm{d}} \neq 0$, is the zero torque locus, highlighted in Fig. 6(a). Along this trajectory, the PM and reluctance effects are even, resulting in zero torque:

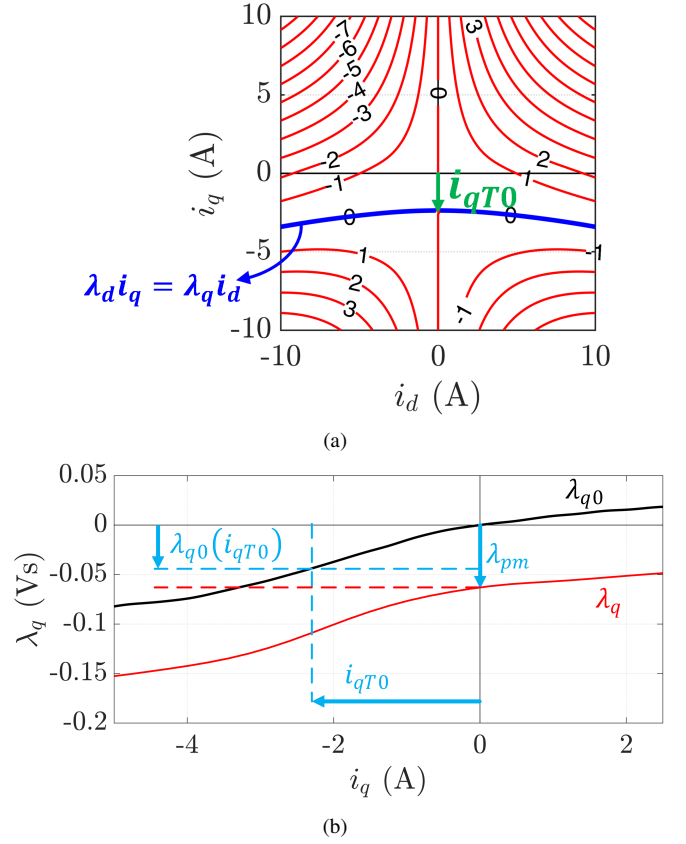$$\lambda_{\mathrm{pm}} = \lambda_{\mathrm{q}0} - \frac{\lambda_{\mathrm{d}} i_{\mathrm{q}}}{i_{\mathrm{d}}} \qquad (12)$$

Fig. 6(a) shows the zero torque locus in the dq plane. Eq. (12) can be applied to any point of this line to obtain an estimation of λ_{pm}. However, it is convenient to apply (12) to the singular point $(i_{\mathrm{d}} = 0, i_{\mathrm{q}} = i_{\mathrm{qT0}})$, defined as the intercept between the zero torque locus and the q axis:

$$\lambda_{\mathrm{pm}} = \lim_{\substack{i_{\mathrm{d}} \to 0 \\ i_{\mathrm{q}} \to i_{\mathrm{qT0}}}} \left(\lambda_{\mathrm{q}0} \left(i_{\mathrm{q}} \right) - \frac{\lambda_{\mathrm{d}} i_{\mathrm{q}}}{i_{\mathrm{d}}} \right)$$
$$= \lambda_{\mathrm{q}0} \left(i_{\mathrm{qT0}} \right) - L_{\mathrm{d}} i_{\mathrm{qT0}} \qquad (13)$$

Fig. 6(b) explains the application of (13). Since $i_{\mathrm{d}} \to 0$, the apparent inductance $L_{\mathrm{d}} = \frac{\lambda_{\mathrm{d}}}{i_{\mathrm{d}}}\big|_{id \to 0}$ can be conveniently evaluated from test #1 in the linear region of $\lambda_{\mathrm{d}}(i_{\mathrm{d}})$ curve, while $\lambda_{\mathrm{q}0}(i_{\mathrm{q}})$ is obtained from test #2. Therefore, at this point of the procedure the only missing parameter to evaluate λ_{pm} is the key current i_{qT0}. [13] proposed to evaluate i_{qT0} from a sequence of rotor alignment. A novel procedure is defined here, performed at standstill whatever the mechanical load.

V. Analysis of $\lambda_{\mathrm{q}}(i_{\mathrm{q}})$ Characteristic

Before describing the method, the shape of $\lambda_{\mathrm{q}}(i_{\mathrm{q}})$ curve must be analyzed. As can be seen in Fig. 5(b), this curve is almost linear for every current value except a restricted area at negative i_{q} where a sharp rate change occurs. This strong
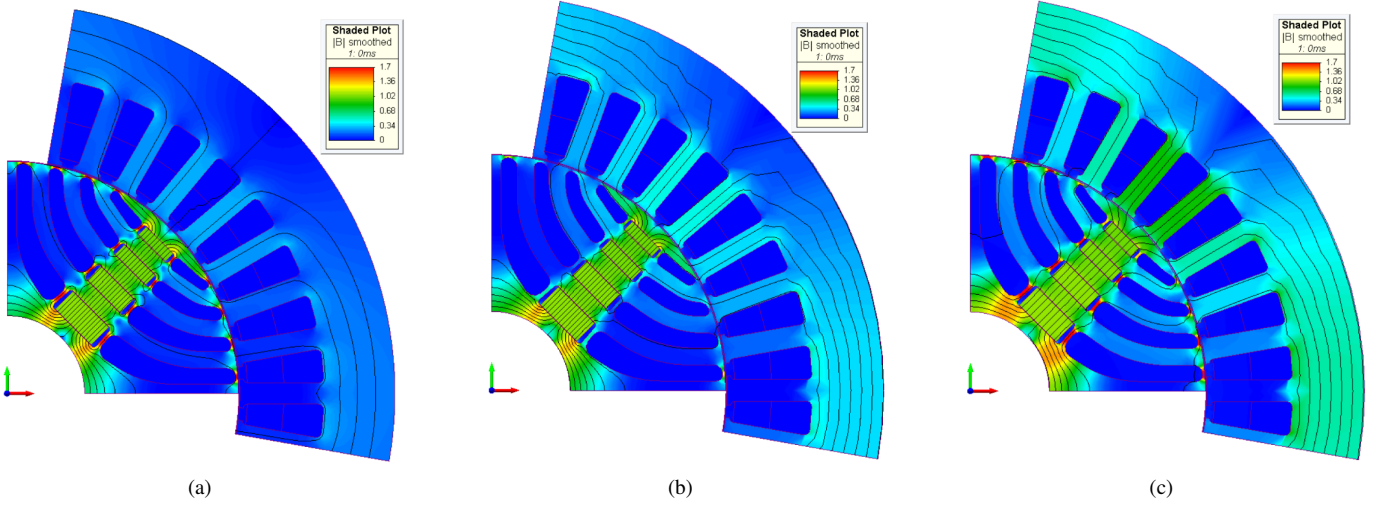
(a)   (b)   (c)

Fig. 7. Finite Element Analysis for the PM-SyR machine under test. (a) zero current ($i_{\rm d}$=0,$i_{\rm q}$=0); (b) minimum saliency point ($i_{\rm d}$=0,$i_{\rm q} = i'_{\rm qT0}$); (c) below the knee ($i_{\rm d}$=0,$i_{\rm q}$=-7 A).

inductance variation is related to de-saturation of the rotor structural ribs.

For null or positive $i_{\rm q}$ the ribs are saturated and the differential inductance $l_{\rm q}$ is almost constant. At negative current, the armature and PM flux components have opposite effects on the ribs, so for sufficiently high negative $i_{\rm q}$ the saturation is lost. In this condition, the flux can linearly pass through the machine also in q axis, so $l_{\rm q}$ is almost equal to $l_{\rm d}$ and the saliency drastically drops. If the negative $i_{\rm q}$ is further increased, the flux contribution due to $i_{\rm q}$ overcomes $\lambda_{\rm pm}$, thus saturating the ribs in the opposite direction respect to the one imposed by the PM. Beyond this point, the curve is again linear.

The basic assumption behind the method proposed here is that the current $i_{\rm qT0}$ is nearly equal to the current corresponding to maximum $l_{\rm q}$, which from here on will be called $i'_{\rm qT0}$. In other words, the curve $\lambda_{\rm q}(i_{\rm q})$ presents its maximum slope approximately at $\lambda_{\rm q}(i_{\rm qT0})$. It must be noted that this condition also corresponds to the minimum local saliency along the q axis.

To demonstrate this assumption is rather critical analytically, since in that area the machine behavior is strongly non-linear and any assumption to simplify the analysis would fail. Anyway, the correspondence between $i_{\rm qT0}$ and $i'_{\rm qT0}$ has been verified based on the experimental flux maps of several PM-SyR motors. For each of them, the discrepancy between $i_{\rm qT0}$ and $i'_{\rm qT0}$ was lower than 3 % of the rated current.

For better explaining the concept, Fig. 7 represents the magnetic density plot of one pole of the PM-SyR machine under test obtained with accurate Finite Element Analysis (FEA). The FEA simulation is executed three times. In Fig. 7(a), the stator current is zero. In this case, the PM saturate the structural ribs, leading to $l_{\rm d} >> l_{\rm q}$. In Fig. 7(b), the minimum saliency point of the q axis was simulated, i.e. $i_{\rm d}$=0 while $i_{\rm q} = i'_{\rm qT0}$. As can be seen, in this condition the structural ribs are not saturated, and so the magnetic flux can linearly flow either in d and q direction. As a result, the reluctance along d

and q axes is nearly the same and so $l_{\rm d} \approx l_{\rm q}$. In Fig. 7(c) the negative $i_{\rm q}$ was further increased ($i_{\rm q}$=-7 A). It can be noted that the ribs are saturated again, so $l_{\rm d} >> l_{\rm q}$, but differently from Fig. 7(a) the saturation is due to the current, instead of the PM.

VI. DETERMINATION OF $i_{\rm qT0}$ BASED ON MINIMUM SALIENCY

If $i_{\rm qT0} \approx i'_{\rm qT0}$ is assumed, the latter can be used in place of $i_{\rm qT0}$ in (13) for evaluating $\lambda_{\rm pm}$:

$$\lambda_{\rm pm} \approx \lambda_{\rm q0}\left(i'_{\rm qT0}\right) - L_{\rm d}i'_{\rm qT0} \tag{14}$$

A dedicated test is proposed to evaluate $i'_{\rm qT0}$, as described in the following.

A. Saliency Evaluation Test

Again, the rotor position does not change during the test so $\hat{\theta}_0$ is adopted for dq frame definition.

The motor control scheme is report in Fig. V. A fundamental DC current vector is forced in negative q axis through a simple PI based current control loop ($i_{\rm d}^* = 0$). At the meantime, a HF rotating voltage component $\boldsymbol{v}_{\rm dqh}$ is superimposed to the fundamental excitation.
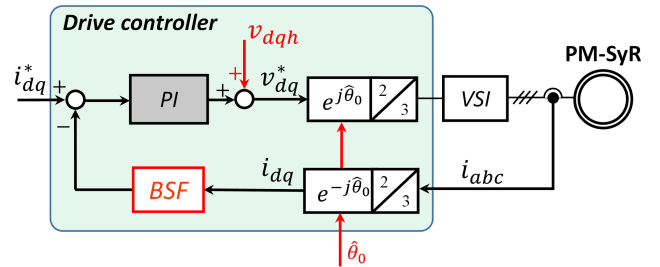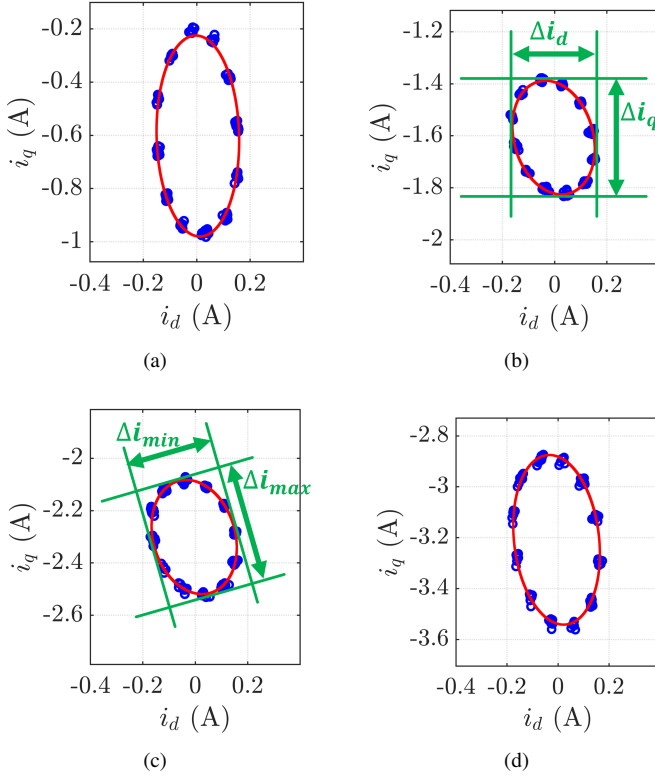

Fig. 8. Block diagram for local saliency evaluation.

Fig. 9. Saliency analysis along the q axis with a HF rotating voltage superimposed to a DC excitation of (a) $i_\mathrm{q} = -0.6$ A, (b) $i_\mathrm{q} = -1.6$ A (c) $i_\mathrm{q} = -2.3$ A (d) $i_\mathrm{q} = -3.2$ A. Blue: measurement points. Red: fitting curve.
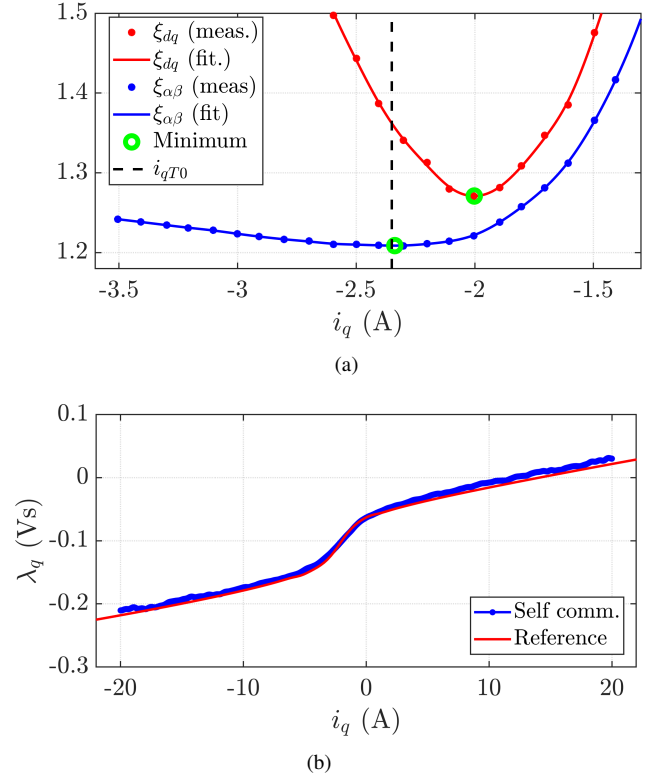

Fig. 10. (a) Evaluated saliency along q axis with (blue) or without (red) considering ellipse rotation. Black dashed line: reference i_qT0. (b) Final $\lambda_\mathrm{q}(i_\mathrm{q})$ characteristic obtained from stand-still self-commissioning.

$$\begin{cases} v_\mathrm{dh} &= u_\mathrm{c} cos\left(2\pi f_\mathrm{c} t\right) \\ v_\mathrm{qh} &= u_\mathrm{c} sin\left(2\pi f_\mathrm{c} t\right) \end{cases} \qquad (15)$$

where u_c and f_c are the amplitude and frequency of the injected voltage. According to the HF model described in Section II-B, the HF current response can be evaluated as:

$$\begin{cases} i_\mathrm{dh} &= \frac{u_\mathrm{c}}{2\pi f_\mathrm{c} l_\mathrm{d}} sin\left(2\pi f_\mathrm{c} t\right) \\ i_\mathrm{qh} &= -\frac{u_\mathrm{c}}{2\pi f_\mathrm{c} l_\mathrm{q}} cos\left(2\pi f_\mathrm{c} t\right) \end{cases} \qquad (16)$$

Therefore, the HF current response describes an elliptic trajectory, and the eccentricity of the ellipse indicates the local saliency.

The reference fundamental current vector is slowly moved along negative q-axis, permitting to evaluate the local anisotropy and thus finding i'_qT0.

It should be noted that in this test the motor is excited along the PM direction. Therefore, even at free shaft and/or in case of inaccurate initial position estimation $\hat{\theta}_0$ the test cannot provoke any rotor movement.

Fig. 9 shows the current trajectories in the dq plane in some key points and defines the quantities Δi_d, Δi_q, Δi_{min} and Δi_{max}.

B. Methods for Extracting i'_qT0

As a first attempt, the machine saliency can be evaluated as the ratio between the maximum HF current elongation in d and q axes, called Δi_d and Δi_q respectively:

$$\xi_{dq} = \frac{\Delta i_\mathrm{q}}{\Delta i_\mathrm{d}} \qquad (17)$$

Following this approach, the red curve of Fig. 10(a) was obtained. As can be seen, this method resulted unreliable for determining i'_qT0. A different strategy is proposed here.

Looking at Fig. 9, an unexpected phenomenon was observed: along the negative i_q axis, the current ellipse is slightly rotated respect to the dq coordinates. To take into account the ellipse rotation, the saliency must be evaluated as the ratio between the ellipse major and minor axes:

$$\xi_{\alpha\beta} = \frac{\Delta i_{max}}{\Delta i_{min}} \qquad (18)$$

Following this approach, i'_qT0 is accurately retrieved (blue line in Fig. 10(a)) and its value (-2.337 A) results very close to i_qT0 (-2.35 A).

Finally, λ_pm is evaluated based on (13), obtaining an error in λ_pm estimation of -0.42 %. The obtained $\lambda_\mathrm{q}(iq)$ characteristic is report in Fig. 10(b).

VII. CONCLUSION

The main contribution of this work is the evaluation of λ_{pm} at standstill and without necessity of position transducers. The proposed techniques relies on machine local anisotropy along negative q axis, evaluated through HF excitation test and proper post-processing manipulation. This test completes the standstill self-commissioning procedure [9] extending the results to PM-SyR machines. Overall, the complete flux maps of PM-SyR machines are retrieved at standstill, without locking the rotor and encoderless. Accurate experimental results were obtained, with relative error lower than 0.5%.

REFERENCES

[1] N. Bianchi, E. Fornasiero and S. Bolognani, "Effect of Stator and Rotor Saturation on Sensorless Rotor Position Detection," in *IEEE Transactions on Industry Applications*, vol. 49, no. 3, pp. 1333-1342, May-June 2013.

[2] D. Paulus, P. Landsmann and R. Kennel, "Sensorless field- oriented control for permanent magnet synchronous machines with an arbitrary injection scheme and direct angle calculation," 2011 Symposium on Sensorless Control for Electrical Drives, Birmingham, 2011, pp. 41-46.

[3] S. Ichikawa, M. Tomita, S. Doki and S. Okuma, "Sensorless Control of Synchronous Reluctance Motors Based on Extended EMF Models Considering Magnetic Saturation With Online Parameter Identification," in IEEE Transactions on Industry Applications, vol. 42, no. 5, pp. 1264-1274, Sept.-Oct. 2006.

[4] IEEE, "1812-2014 - IEEE Trial-Use Guide for Testing Permanent Magnet Machines.", 2015.

[5] S. A. Odhano, P. Pescetto, H. A. A. Awan, M. Hinkkanen, G. Pellegrino, and R. Bojoi, "Parameter identification and self-commissioning in ac motor drives: a technology status review," *IEEE Transactions on Power Electronics*, 2018.

[6] S. Yang and K. Lin, "Automatic control loop tuning for permanent magnet ac servo motor drives," IEEE Transactions on Industrial Electronics, 2016.

[7] L. Peretti, P. Sandulescu and G. Zanuso, "Self-commissioning of flux linkage curves of synchronous reluctance machines in quasi-standstill condition," in *IET Elect. Pow. Appl.*, 2015.

[8] N. Bedetti, S. Calligaro, and R. Petrella, "Stand-still self-identification of flux characteristics for synchronous reluctance machines using novel saturation approximating function and multiple linear regression," *IEEE Trans. on Ind. App.*, 2016.

[9] M. Hinkkanen, P. Pescetto, E. Molsa, S. E. Saarakkala, G. Pellegrino, and R. Bojoi, "Sensorless self-commissioning of synchronous reluctance motors at standstill without rotor locking," *IEEE Trans. on Ind. App.*, May 2017.

[10] T. Tuovinen, H. A. Ali Awan, J. Kukkola, S. E. Saarakkala and M. Hinkkanen, "Permanent-Magnet Flux Adaptation for Sensorless Synchronous Motor Drives," 2018 *IEEE 9th International Symposium on Sensorless Control for Electrical Drives (SLED)*, Helsinki, 2018, pp. 138-143.

[11] Z. Q. Zhu, X. Zhu, P. D. Sun and D. Howe, "Estimation of Winding Resistance and PM Flux-Linkage in Brushless AC Machines by Reduced-Order Extended Kalman Filter," 2007 *IEEE International Conference on Networking, Sensing and Control*, London, 2007, pp. 740-745.

[12] S. A. Odhano, P. Giangrande, R. I. Bojoi and C. Gerada, "Self-Commissioning of Interior Permanent- Magnet Synchronous Motor Drives With High-Frequency Current Injection," in *IEEE Transactions on Industry Applications*, vol. 50, no. 5, pp. 3295-3303, Sept.-Oct. 2014.

[13] P. Pescetto and G. Pellegrino, "Sensorless magnetic model and PM flux identification of synchronous drives at standstill," *2017 IEEE International Symposium on Sensorless Control for Electrical Drives (SLED)*, 2017.

[14] J. Jacob, P. Kumar, S. Calligaro, and R. Petrella, "Self-commissioning identification of permanent magnet flux-linkage magnitude in sensorless drives for PMSM at quasi stand-still," in *2018 IEEE 9th International Symposium on Sensorless Control for Electrical Drives (SLED)*, 2018.

[15] P. Pescetto and G. Pellegrino, "Automatic Tuning for Sensorless Commissioning of Synchronous Reluctance Machines Augmented With High-Frequency Voltage Injection," in *IEEE Transactions on Industry Applications*, vol. 54, no. 5, pp. 4485-4493, Sept.-Oct. 2018.